

Single Fe₂B Phase Particle Production by Calciothermic Reduction in Molten Salt

Levent Kartal¹ 

¹Hitit University, Department of Metallurgical and Materials Engineering, Corum, Turkey

ABSTRACT

In this study, calciothermic single phase iron boride(Fe₂B) production was investigated in a scalable molten salt system, starting from inexpensive, easily accessible oxide materials. First, the formation of Fe₂B was examined in detail in the light of thermodynamic data and literature. After, effects of CaO amount (0-10 wt.%) and time (30-60 min) on particle synthesis were investigated under at constant 3.0 V cell voltage and 1273 K temperature. It was determined that the average current increased continuously with the increase in the amount of CaO, and the current efficiency increased up to 7% by weight of CaO. After the CaO ratio was determined, the effect of the electrolysis duration was examined. In durations experiments, it has been observed that, in 30 minutes' duration, the particles are composed of Fe, Fe₂B and FeB, and by increasing the experiment time to 60 min, single-phase Fe₂B particles are obtained. The magnetic properties of the single-phase Fe₂B particles obtained at the end of the experiment period of 60 minutes were investigated by VSM. The saturation magnetization, permanent magnetization and coercivity values of the Fe₂B particles were determined as 90.718 emu/g, 33.311 Oe, 1.684 emu/g, respectively.

Keywords:

Molten salt electrolysis; Iron boride; Calciothermic reduction; Borides.

INTRODUCTION

Transition metal borides are widely used in different applications due to their high melting temperature, high hardness, high corrosion and wear resistance, good chemical stability, high electrical and thermal conductivity. Among metal borides, iron borides (Fe_xB) draw attention with their superior performance and wide usage area, especially on metallic surfaces with boriding. Besides to boronization, B additive in steels is also made with FeB particles. In addition to iron and steel applications, iron borides are also used in many areas such as powder metallurgy, magnetic material, catalysts and metal-air battery applications due to their superior physical and chemical properties [1-3].

Mass production of Fe_xB particles is carried out by carbothermic reduction of oxide raw materials in electric arc furnaces. Although the carbothermic method is a simple procedure for mass production, it consumes a lot of energy and emits greenhouse gases [4]. Reaching the irreversible point of global warming requires the removal of fossil fuels, which cause high greenhouse gas emissions, from production processes. To reduce greenhouse gas emissions FeB production was studied by metallothermic (aluminothermic) reduction of oxide

raw materials. Although it is possible to produce with low energy and greenhouse gas with aluminothermic reduction, Al residues seen in the product could not be completely removed [5]. In addition to the aforementioned methods, FeB production can be made starting from semi-finished raw materials for low-volume specialized applications. The most widely used of these methods are solid state reaction of Fe and B, chemical reduction, mechanical alloying, molten salt electrolysis and metallothermic reduction processes[1, 2, 6-9].

Production of metal borides with low energy and low greenhouse gas emission from cheap oxidized components is also possible with metallothermic and molten salt electrolysis methods. In particular, metallothermic methods come to the fore with the possibility of high-speed production. Metallothermic metal boride production is generally carried out by reducing metal oxide (MeO) and boron oxide (B₂O₃) with a reductant (Al, Mg, Ca, Y) in a ball mill under a protective atmosphere [10-12]. In this conventional method, oxide powder reduction takes place from outside to inside and a reductant oxide film is formed at the MeO/Me interface. The reducing oxide film thickening over time at the Me/MeO interface may slow down the reduction and cause

Article History:

Received: 2022/04/22

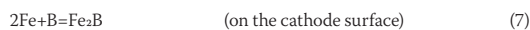
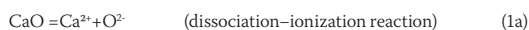
Accepted: 2022/06/20

Online: 2022/06/30

Correspondence to: Levent Kartal,
Hitit University, Department of
Metallurgical and Materials Engineering,
19030, Corum, Turkey
E-Mail: leventkartal@hitit.edu.tr
Phone: +90 (364) 219 1200
Fax: +90 (364) 219 3320

the vapor pressure of CaCl_2 , which constitutes the majority of the electrolyte, and the melting points of the Fe_xB compounds targeted to be produced. Mixing is an important factor that is neglected but increases the process efficiency and duration by reducing the diffusion layer at the cathode boundary. Mixing can be done by different methods such as mechanical, ultrasonic and etc.,. In this study, induction was preferred for heating the cell, and the mixing feature of induction was also utilized [19].

The calciothermic synthesis of Fe_2B in a molten salt takes place in 2 steps. First, Fe_2O_3 with low thermodynamic stability is reduced by Ca, then the B adhere to the surface of Fe and form Fe_xB particles. Due to its low melting temperature, B_2O_3 is molten and in full mixture with CaCl_2 under experimental conditions. CaO can be dissolved up to 20% by mole in CaCl_2 . CaCl_2 was preserved within the CaO dissolving limits by adding 7 wt.% CaO, and a homogenous electrolyte was created [15, 20]. By applying voltage, CaO in contact with the large cathode surface is reduced and Ca is produced (eq. 1b). In CaCl_2 , 4% of the calcium generated can be dissolved [18]. After adding Fe_2O_3 (5.24 g/cm^3) accumulates at the bottom of the crucible due to its density. Dissolved Ca reacts with Fe_2O_3 particles in a large surface area and performs Fe_2O_3 reduction [21]. While the reduction of Fe_2O_3 occurs in a large surface area with Ca dissolved in the electrolyte, it also occurs electrochemically from a narrow surface area where it comes into contact with the cathode from the moment the current is applied (eq. 2). Fe (7.874 g/cm^3) particles produced as a result of cathodic and calciothermic reduction form the new cathode surface by accumulating at the bottom of the graphite crucible due to its density. Elemental B is formed by the reduction of B_2O_3 by Ca at the Fe electrolyte interface, and B diffuses into Fe particles with the driving force of concentration gradient and temperature (eq. 6, 7). Thermodynamically, the first product formed on the Fe surface by B diffusion is always the boride compound (Fe_2B) with the lowest mole fraction of boron (eq. 7). Fe_2B turns into FeB with the increase of B amount and diffusion on the Fe_2B surface (eq. 8a). With sufficient duration allowed for B diffusion, Fe_2B turns into FeB, while FeB reacts with Fe at the particle center to form Fe_2B again (eq. 8b). A small amount of CaB_6 formation in the cell seems also likely (eq. 9, fig 2). Due to the use of graphite anodes, CO and CO_2 gases are expected to form on the anode (equation 3, 4) [22].



Decomposition potentials (ΔE) of the components were calculated from the Gibbs free energy of formation (ΔG) values of components. The decomposition potentials (ΔE) of the materials used were calculated using Eq. 1. In Eq. 1, n represents the number of electrons and F represents Faraday's constant.

$$\Delta E = -\Delta G / (nF) \quad (10)$$

The temperature dependent decomposition potentials of the probable reaction couples expected to take place within cells under the experimentation conditions are given in Figure 2. The decomposition voltage of CaO was determined to be approximately 1.0V lower than its theoretical value while using a carbon anode (Fig. 2). The low decomposition voltage of CaO eliminated the risk of $\text{Cl}_2(\text{g})$ emission and permitted the opportunity for calciothermic reduction under a wide range of potentials below the CaCl_2 decomposition voltage.

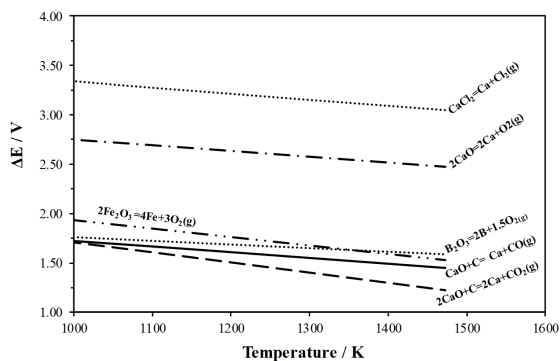


Figure 2. Change in the decomposition potentials (ΔE) for CaCl_2 , CaO, and Fe_2O_3 as a function of temperature

In processes where formation of more than one compound is possible, change of Gibbs free formation energies of reactions are used in product estimation. The Gibbs free formation energies of the compounds that can be formed in the light of the reactions taking place in the cell, which change with temperature, are calculated with the help of the HSC Chemistry 5.1 version and given in figure 3. When the graph in Figure 3 is examined, it is understood that the first compound to be formed is Fe_2B . While FeB formation is expected to occur with a lower probability than Fe_2B , it is seen that the lowest expected formation is CaB_6 .

Effect of CaO Amount on Current

In this study $\text{CaCl}_2/\text{CaO}/\text{B}_2\text{O}_3$ mixture was employed as

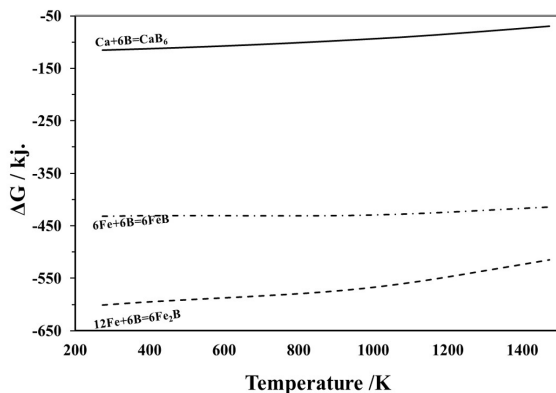


Figure 3. Change in Gibbs free energy of boron, calcium and iron reactions as a function of temperature as a function of temperature.

an electrolyte which mostly contained CaCl_2 . Because of its complete molten state at the reaction temperature, the amount of B_2O_3 was held constant. Because of its restricted solubility in CaCl_2 , impact on solution viscosity, and impact on oxygen content of the product via increased oxygen activity in the electrolyte, CaO was the most important ingredient in the electrolyte. Low amounts of CaO resulted in insufficient reduction, whereas too much CaO resulted in very high CaO activity and produced a very high oxygen content in the product. The impact of the amount of CaO on Fe_xB production was examined over a range of 0 to 10 wt.% of CaO under a constant cell voltage of 3.0 V at a reaction temperature of 1273 K for 30 minutes. The current changes depending on the CaO ratios are given in figure 4. The average current value increased with increased CaO , while the change trends were similar for different durations of experimentation [17]. The increase in the initial current value with increased CaO concentration indicated more Ca production in the electrolyte. For low amounts of added CaO the current dropped after a very short time owing to the easy reduction of CaO . However, adding 7 wt.% of CaO – or higher concentrations – made this reduction slower and more gradual. High CaO content provided a high current regime within the electrolyte. High CaO was reported to reduce the dissolution of CaO in the vicinity of cathode by forming concentrated CaO regions, and this can prevent the cathodic reactions [23]. Additionally, high CaO also considerably reduced the solubility of Ca [21]. It was discovered that as the amount of CaO rose, the cathode products produced grew by 7% and reduced by 10% in weight. Considering the solubility limits of CaO in CaCl_2 , amount of cathode product, the literature and the current values obtained, it was decided to use 7 wt.% CaO for the experiments.

The fixed percentage of CaO used in the experiments was decided by considering the current efficiencies obtained in the experiments performed with different CaO amounts. The current efficiencies, which vary according to the

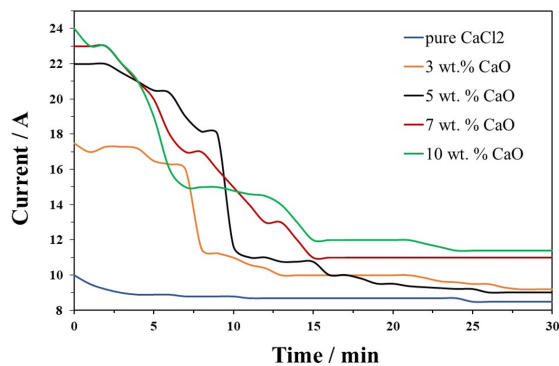


Figure 4. Current time curves obtained during electrolysis at 1273 K with a constant potential of 3.0 V for 30 minutes.

amount of CaO , are calculated over the theoretical amount of Ca that should be produced with the current used and the amount of Ca used for the amount of product produced.

The current efficiencies obtained at different CaO ratios are given in Figure 5. It was observed that as the amount of CaO rose, the efficiencies grew by 7% and reduced by 10% in weight. Considering the solubility limits of CaO in CaCl_2 , amount of cathode product, the literature and the current values obtained, it was decided to use 7 wt.% CaO for the experiments.

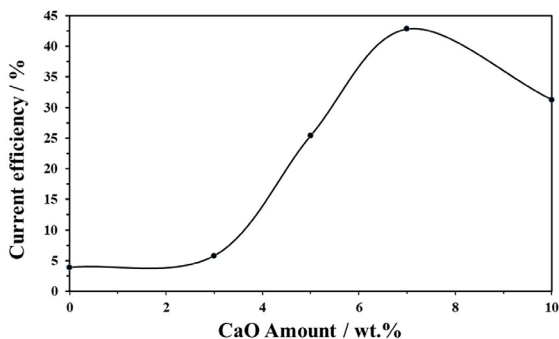


Figure 5. Variations of current efficiency versus CaO amount.

Effect of Process Duration on Fe_xB Synthesis

Considering the experimental conditions and the materials used, the maximum temperature and voltage were selected, and the effect of the time was examined. The phase structure of the particles obtained at different times was examined by XRD analysis, and the XRD patterns are given in figure 6. XRD results revealed that 30 min is not sufficient for B diffusion and single-phase particle structure, due to the presence of Fe , Fe_2B and FeB phases. The experiment was repeated under the same conditions by extending the experiment duration to 60 min, and unlike 30 min, it was observed that the particles consisted of a single Fe_2B phase.

The morphology of the particles obtained at different durations were examined by SEM (fig. 7). While there was

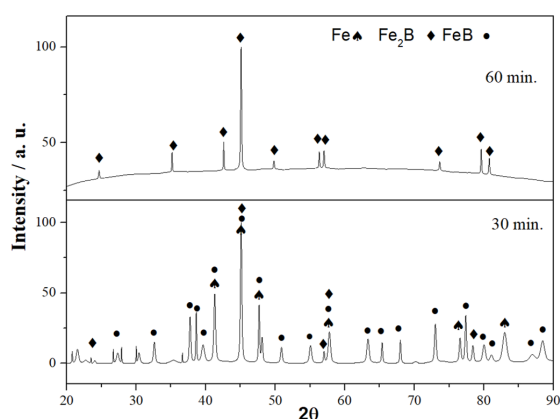


Figure 6. XRD patterns of Fe₂B powders produced at different durations at constant 3.0 V cell voltage.

no big difference in morphology over time in the particles given in Figure 7, it was observed that the particle morphologies were polygonal. Similar particle morphologies have been seen in metallothermic reactions carried out in various conditions [24][25].

The magnetic behaviours of Fe₂B particles produced at under 1273 K temperature for 60 minutes' conditions were examined at room temperature. From the magnetization curve given in Figure 8, it was determined that it showed a soft magnetic behaviour under the magnetic field and had hysteresis like ferrimagnetism. The powders had a saturation magnetization value of $M_s=90.818$ emu/g, a coercive magnetization value of $M_c=33.311$ Oe, and a remanent magnetization value of $M_r=1.684$ emu/g, according to the results.

CONCLUSION

In this study, it has been shown that calciothermic Fe₂B can be produced in one step from technical purity quality, inexpensive, easily accessible materials without the need for pre-and post-treatment. Experiments were carried out using CaCl₂-CaO-B₂O₃-Fe₂O₃ electrolyte under constant 1273 K temperature and 3.0 V cell potential conditions for 30 and 60 min. The experimental results obtained are summarized as follows;

a) The formation of single-phase Fe₂B was examined in detail in the light of thermodynamic and experimental data, and it was determined that the conversion of Fe₂O₃ to Fe₂B would take place in the order of Fe-FeB-Fe₂B.

b) The influence of the amount of CaO on current was examined over a range of 0 to 10 wt.% of CaO under a constant cell voltage of 3.0 V at a reaction temperature of 1273 K for 30 minutes. It was observed that the current value increased continuously with the increase in CaO and reached 24 A at the amount of 10 wt. % CaO.

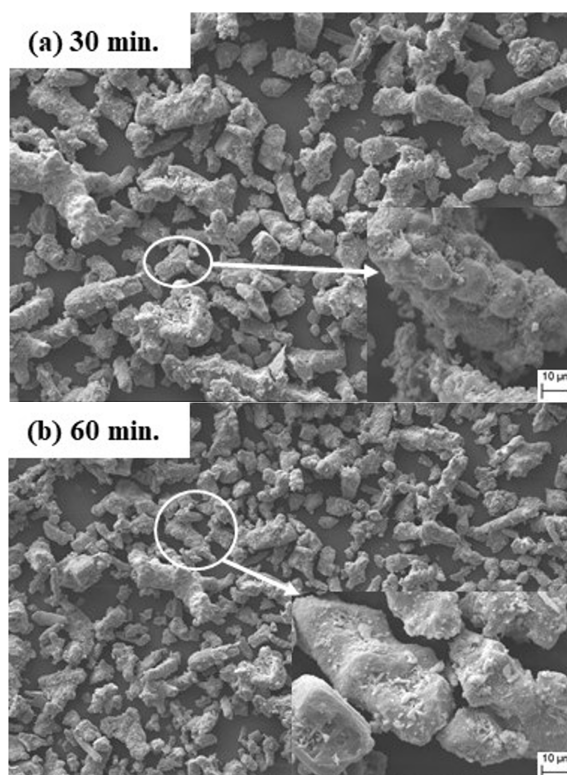


Figure 7. Current variations versus time and SEM images of Fe₂B powders produced at different durations at constant 3.0 V cell voltage.

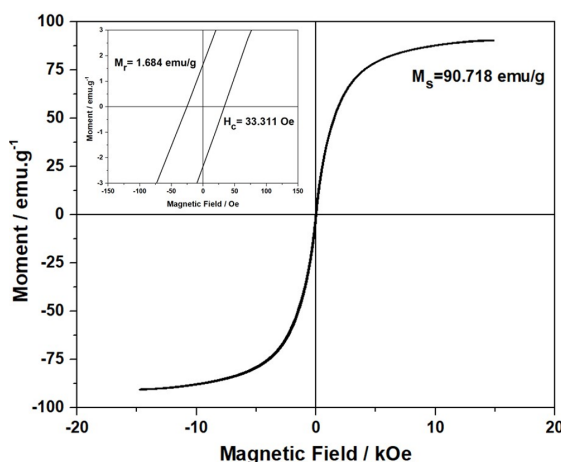


Figure 8. Magnetization curves of Fe₂B powders produced at constant 1273 K temperature and cell voltage of 3.0 V for 60 min durations.

c) The effect of the time was examined by performing experiments at 30-60 min., single-phase particles could not be obtained in 30 min. It was determined that the particles consisted of Fe, Fe₂B and FeB phases. With the increasing of the time to 60 min, it was shown that Fe and FeB structures contained in the particle were turned into Fe₂B.

d) The magnetic properties of the Fe₂B particles produced at 1273 K temperature, 3.0 V cell voltage for 60 minutes were investigated under room temperature conditions in the range of 0-1.5 T. The saturation magnetization, perma-

ment magnetization and coercivity values of the Fe₂B particles obtained at the end of the 60 min experiment period were determined as 90.718 emu/g, 33.311 Oe, 1.684 emu/g, respectively.

CONFLICT OF INTEREST

The authors declare that they have no known competing financial interests or personal relationships that could have appeared to influence the work reported in this paper.

References

1. Wei Y, Liu Z, Ran S, Xia A, Yi TF, Ji Y. Synthesis and properties of Fe-B powders by molten salt method. *Journal of Materials Research* 32(4) (2017) 883–889.
2. Mohammadi M, Ghasemi A, Tavooosi M. Mechanochemical synthesis of nanocrystalline Fe and Fe-B magnetic alloys. *Journal of Magnetism and Magnetic Materials* 419 (2016) 189–197.
3. Hamayun MA, Abramchuk M, Alnasir H, Khan M, Pak C, Lenhart S, et al. Magnetic and magnetothermal studies of iron boride (FeB) nanoparticles. *Journal of Magnetism and Magnetic Materials* 451 (2018) 407–413.
4. Verma PC, Mishra SK. Synthesis of iron boride powder by carbothermic reduction method. *Materials Today: Proceedings* 28 (2019) 902–906.
5. Yücel O, Cinar F, Addemir O, Tekin A. The preparation of ferroboration and ferrovanadium by aluminothermic reduction. *High Temperature Materials and Processes* 15(1–2) (1996) 103–109.
6. Barış M, Şimşek T, Taşkaya H. Synthesis of Fe-Fe₂B catalysts via solvothermal route for hydrogen generation by hydrolysis of NaBH₄. *Journal of Boron* 3(1) (2018) 51–62.
7. Abenojar J, Velasco F, Mota JM, Martínez MA. Preparation of Fe/B powders by mechanical alloying. *Journal of Solid State Chemistry* 177(2) (2004) 382–388.
8. Ozkalafat P, Sireli GK, Timur S. Electrodeposition of titanium diboride from oxide based melts. *Surface and Coatings Technology* 308 (2016) 128–135.
9. Simsek T, Baris M, Kalkan B. Mechanochemical processing and microstructural characterization of pure Fe₂B nanocrystals. *Advanced Powder Technology* 28(11) (2017) 3056–3062.
10. Kudaka K, Iizumi K, Izumi H, Sasaki T. Synthesis of titanium carbide and titanium diboride by mechanochemical displacement reaction. *Journal of Materials Science Letters* 20(17) (2001) 1619–1622.
11. Kim JW, Shim JH, Ahn JP, Cho YW, Kim JH, Oh KH. Mechanochemical synthesis and characterization of TiB₂ and VB₂ nanopowders. *Materials Letters* 62(16) (2008) 2461–2464.
12. Radev DD, Marinov M. Comparative studies on the high-temperature and mechanochemical synthesis of titanium diboride. *Comptes Rendus de L'Academie Bulgare des Sciences* 66(6) (2013) 827–832.
13. Okabe TH. Metallurgical reduction of TiO₂ in: Fang ZZ, Froes FH, Zhang Y(Eds.). *Extractive Metallurgy of Titanium*. Elsevier, Amsterdam, pp.131–164, 2020
14. Descallar-Arriesgado RF, Kobayashi N, Kikuchi T, Suzuki RO. Calciothermic reduction of NiO by molten salt electrolysis of CaO in CaCl₂ melt. *Electrochimica Acta* 56(24) (2011) 8422–8429.
15. Suzuki RO. Direct reduction processes for titanium oxide in molten salt. *JOM* 59(1) (2007) 68–71.
16. Ono K, Okabe TH, Suzuki RO. Design, test and theoretical assessments for reduction of titanium oxide to produce titanium in molten salt. *Materials Transactions* 58(3) (2017) 313–318.
17. Suzuki RO. Calciothermic reduction of TiO₂ and in situ electrolysis of CaO in the molten CaCl₂. *Journal of Physics and Chemistry of Solids* 66(2–4) (2005) 461–465.
18. Ağağüllari D, Balci Ö, Duman İ, Mechanisms and effects of various reducing agents on the fabrication of elemental boron. *Metal* (2010) 18–23.
19. Sireli GK. Molten salt baths: Electrochemical boriding. in: Colás R, Totten GE (Eds.). *Encyclopedia of Iron, Steel, and Their Alloys*. Taylor and Francis, Boca Raton, pp. 2284–2300, 2016
20. Zaitsev AI, Mogutnov BM, Thermodynamics of the Ca-CaO-CaF₂ System. *Metallurgical and Materials Transactions B* 32 (2001) 305–311.
21. Suzuki RO, Natsui S, Kikuchi T. OS process: Calciothermic reduction of TiO₂ via CaO electrolysis in molten CaCl₂, in: Fang ZZ, Froes FH, Zhang Y(Eds.). *Extractive Metallurgy of Titanium*. Elsevier, Amsterdam, pp.287–313, 2020
22. Suzuki RO, Ono K, Teranuma K. Calciothermic reduction of titanium oxide and in-situ electrolysis in molten CaCl₂. *Metall Mater Trans B* 34 (2003) 287–95.
23. Abdelkader AM, Daher A, Abdelkareem RA, El-Kashif E. Preparation of zirconium metal by the electrochemical reduction of zirconium oxide. *Metall Mater Trans B Process Metall Mater Process Sci* 38 (2007) 35–44.
24. Şimşek T, Özcan S. Fabrication and Characterization of Mn₂B Nanoparticles by Mechanochemical Method. *Journal of Boron* 4(1) (2019) 25–30.
25. Kovalev DY, Potanin AY, Levashov EA, Shkodich NF. Phase formation dynamics upon thermal explosion synthesis of magnesium diboride. *Ceramics International* 42(2) (2016) 2951–2959.